Supplemental Material for "Nanofluidic osmotic diodes: theory and molecular dynamics simulations"

Clara B. Picallo,[1] Simon Gravelle,[1] Laurent Joly,[1,*] Elisabeth Charlaix,[2] and Lydéric Bocquet[1,3,4]

[1]*Institut Lumière Matière, UMR5306 Université Lyon 1-CNRS, Université de Lyon 69622 Villeurbanne, France*
[2]*Laboratoire interdisciplinaire de Physique, UMR5588 Université Joseph Fourier-CNRS, 38402 Grenoble, France*
[3]*Department of Civil and Environmental Engineering, Massachusetts Institute of Technology, Cambridge, MA, USA*
[4]*⟨MSE⟩² UMI 3466 CNRS-MIT, Massachusetts Institute of Technology, Cambridge, MA, USA*

(Dated: September 5, 2013)

Contents

ANALYTICAL CALCULATION

We consider here an asymmetrically charged nanochannel of length L and height h, as depicted in Fig. S1. The left side of the channel has a positive surface charge density σ while the right side has a negative surface charge $-\alpha\sigma$, with $\alpha > 1$ a numerical coefficient. Each end of the channel is in contact with a reservoir of concentration $n_L = n_0 - \Delta n/2$ and $n_R = n_0 + \Delta n/2$ in the left and right ends, respectively. A voltage drop $\Delta V = V_R - V_L$ is also applied between the two reservoirs. Three space charge zones (SCZs), denoted by 1, lr, and 2 in figure S1, appear due to the discontinuities of the surface charge: between the reservoirs and the left and right inner ends of the nanochannel, and in the junction between the positively and negatively charged sides of the channel.

For the sake of simplicity, we will use reduced units $\tilde{x} = x/L$, $\tilde{n} = n/n_0$, $\tilde{V} = eV/k_BT$, $j_\pm = JL/Dn_0$ in terms of the length of the system L and the average concentration of the reservoirs n_0. Since we will exclusively use reduced units in the rest of the text, we remove the tildes of the reduced units keeping in mind that in the following, all the variables are dimensionless.

In reduced units, the Nernst-Planck transport equations in the low Peclet number regime read

$$j_\pm = -\nabla n_\pm \mp n_\pm \nabla V \tag{S1}$$

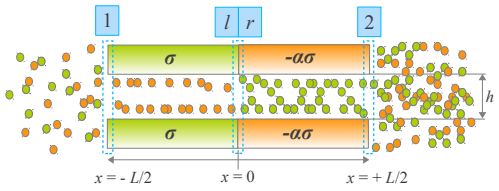

FIG. S1: Sketch of the system showing the three SCZs where the matching conditions are applied.

and give us the fluxes of the negative j_- and the positive j_+ species. The solute j_s and electric j_e fluxes are defined as

$$\begin{aligned} j_s &\equiv j_+ + j_- = -\nabla n_{\text{sol}} - (n_+ - n_-)\nabla V \\ j_e &\equiv j_+ - j_- = -\nabla(n_+ - n_-) - n_{\text{sol}}\nabla V \end{aligned} \tag{S2}$$

in terms of the total ion concentration $n_{\text{sol}} = n_+ + n_-$.

We will also apply a local electroneutrality ansatz. This means that everywhere in the system (out of the SCZs), the positive and negative charges should compensate to give a total zero charge. This gives the following relationship between surface and bulk charges in reduced units,

$$\begin{aligned} n_- - n_+ &= 2\delta, & -1/2 < x < 0 \\ n_+ - n_- &= 2\alpha\delta, & 0 < x < 1/2 \end{aligned} \tag{S3}$$

where δ is the surface-to-bulk charge ratio $\delta = |\Sigma|/hn_0$.

Making use of the electroneutrality condition (S3), the expression for the electric flux j_e in equations (S2) can be further simplified to

$$\begin{aligned} j_s &\equiv j_+ + j_- = -\nabla n_{\text{sol}} - (n_+ - n_-)\nabla V \\ j_e &\equiv j_+ - j_- = -n_{\text{sol}}\nabla V \end{aligned} \tag{S4}$$

We will focus on the minority species on each side of the junction, i.e., n_+ on the left side and n_- on the right side. This means that we will express n_{sol} as

$$n_{\text{sol}} = 2(n_+ + \delta), \qquad -1/2 < x < 0 \tag{S5}$$

$$n_{\text{sol}} = 2(n_- + \alpha\delta), \qquad 0 < x < 1/2 \tag{S6}$$

making use of equations (S3). Furthermore, we will focus on the fluxes $j_+ = (j_s + j_e)/2$ on the left side and $j_- = (j_s - j_e)/2$ on the right side, according to the minority species on each side.

General case

Left side $1/2 < x < 0$*:* Regarding the concentration of the minority species we have

$$j_+ = \frac{1}{2}(j_s + j_e) = -\nabla n_+ - n_+ \nabla V$$

Multiplying both sides of the equation by n_{sol}, recalling that $-n_{\text{sol}}\nabla V = j_e$, substituting n_{sol} by equation (S5) and reorganizing terms, we arrive to the equation

$$j_s(n_+ + \delta(1 + j_e/j_s)) + 2(n_+ + \delta(1 + j_e/j_s) - \delta j_e/j_s)\nabla n_+ = 0, \tag{S7}$$

that can be easily integrated as

$$2n_+ - 2\delta\frac{j_e}{j_s}\log(n_+ + \delta(1 + \frac{j_e}{j_s})) + j_s x = C_{n_+} \tag{S8}$$

where C_{n_+} is a constant of integration.

In order to integrate the voltage we make use of the expression for the electric flux,

$$j_e = -n_{\text{sol}}\nabla V = -2(n_+ + \delta)\nabla V = -2(n_+ + \delta)\nabla_{n_+} V \nabla n_+$$

which, making use of equation (S7) turns,

$$j_e = j_s(n_+ + \delta(1 + j_e/j_s))\nabla_{n_+} V \tag{S9}$$

that can be easily integrated to

$$V = \frac{j_e}{j_s}\log(n_+ + \delta(1 + \frac{j_e}{j_s})) + C_{V_+} \tag{S10}$$

with C_{V_+} a constant of integration.

Right side $0 < x < 1/2$*:* Following the same procedure as for the left side for the minority species, n_- in this case, we arrive to the equation

$$j_s(n_- + \alpha\delta(1 - j_e/j_s)) + 2(n_- + \alpha\delta(1 - j_e/j_s) + \alpha\delta j_e/j_s)\nabla n_- = 0 \tag{S11}$$

that is integrated to

$$2n_- + 2\alpha\delta\frac{j_e}{j_s}\log(n_- + \alpha\delta(1 - \frac{j_e}{j_s})) + j_s x = C_{n_-} \tag{S12}$$

where C_{n_-} is a constant of integration.

Regarding the voltage,

$$j_e = -n_{\text{sol}}\nabla V = -2(n_- + \alpha\delta)\nabla V = -2(n_- + \alpha\delta)\nabla_{n_-} V \nabla n_-$$

which, making use of equation (S11) turns,

$$j_e = j_s\left(n_- + \alpha\delta\left(1 - \frac{j_e}{j_s}\right)\right)\nabla_{n_-} V$$

that integrates to

$$V = \frac{j_e}{j_s}\log\left(n_- + \alpha\delta\left(1 - \frac{j_e}{j_s}\right)\right) + C_{V_-} \tag{S13}$$

with C_{V_-} a constant of integration.

Boundary conditions at the SCZs:

SCZ 1**:** The electroneutrality condition as well as the continuity of the electrochemical potential must hold

$$n_-^1 - n_+^1 = 2\delta \tag{S14}$$
$$\log(1 - \Delta n/2) - \Delta V = \log(n_-^1) + V_1$$
$$\log(1 - \Delta n/2) + \Delta V = \log(n_+^1) + V_1$$

Adding and subtracting the two last equations we obtain respectively,

$$(1 - \Delta n/2)^2 = n_+^1 n_-^1 \tag{S15}$$
$$V_1 = -\Delta V + \frac{1}{2}\log\left(\frac{n_-^1}{n_+^1}\right) \tag{S16}$$

SCZ lr**:** We call l the left side of the junction and r the right side of the junction.We then have,

$$n_-^l - n_+^l = 2\delta$$
$$n_+^r - n_-^r = 2\alpha\delta$$
$$\log(n_-^l) - V_l = \log(n_-^r) - V_r$$
$$\log(n_+^l) + V_l = \log(n_+^r) + V_r$$

Adding and subtracting the two last equations we obtain respectively,

$$\frac{n_-^l}{n_-^r} = \frac{n_+^r}{n_+^l} \tag{S17}$$
$$V_l - V_r = \log\left(\frac{n_+^r}{n_+^l}\right) = \log\left(\frac{n_-^l}{n_-^r}\right) \tag{S18}$$

SZC 2**:** Following the same reasoning as for the SCZ 1,

$$n_+^2 - n_-^2 = 2\alpha\delta \tag{S19}$$
$$\log(1 + \Delta n/2) = \log(n_+^2) + V_2$$
$$\log(1 + \Delta n/2) = \log(n_-^2) - V_2$$

Adding and subtracting the two last equations we obtain respectively,

$$(1 + \Delta n/2)^2 = n_+^2 n_-^2 \tag{S20}$$
$$V_2 = \frac{1}{2}\log\left(\frac{n_-^2}{n_+^2}\right) \tag{S21}$$

Large δ case

If the surface charge dominates over the charge coming from the salt solution, i.e., $\delta \gg 1$, appropriate approximations can be made that allow us to obtain analytical solutions

of the equations. We begin by the electroneutrality conditions (S3) which if $\delta \gg 1$ can be simplified as follows,

$$n_- \simeq 2\delta, \qquad -1/2 < x < 0 \tag{S22}$$
$$n_+ \simeq 2\alpha\delta, \qquad 0 < x < 1/2$$

where, on each side of the junction, only the minority species has a role. This approximation is widespread in the semiconductors literature. Furthermore, if $\delta \gg 1$ we can also approximate equations (S5), (S6) by

$$n_{\text{sol}} \simeq 2\delta, \qquad -1 < 2 < x < 0 \tag{S23}$$
$$n_{\text{sol}} \simeq 2\alpha\delta, \qquad 0 < x < 1/2 \tag{S24}$$

Left side $1/2 < x < 0$*:* Under the condition $\delta \gg 1$, equation (S7) becomes

$$j_s + j_e = -2\nabla n_+, \tag{S25}$$

that is easily integrated to

$$n_+ + \frac{1}{2}(j_s + j_e)x = C_{n_+\delta} \tag{S26}$$

with $C_{n_+\delta}$ a constant of integration. While the voltage equation

$$j_e = -n_{\text{sol}}\nabla V \simeq -2\delta\nabla V \tag{S27}$$

can be integrated as

$$V = \frac{-j_e}{2\delta}x + C_{V_l} \tag{S28}$$

with C_{V_l} a constant of integration.

Right side $0 < x < 1/2$*:* Under the condition $\delta \gg 1$, equation (S11) becomes

$$j_s - j_e = -2\nabla n_- \tag{S29}$$

that can be integrated as

$$n_- + \frac{1}{2}(j_s - j_e)x = C_{n_-\delta} \tag{S30}$$

with $C_{n_-\delta}$ a constant of integration. While the voltage, as before, can be integrated as

$$j_e = -n_{\text{sol}}\nabla V \simeq -2\alpha\delta\nabla V \tag{S31}$$
$$V = \frac{-j_e}{2\alpha\delta}x + C_{V_r} \tag{S32}$$

with C_{V_r} a constant of integration.

Boundary conditions at the SCZs: In the $\delta \gg 1$ case, the boundary conditions are much simpler for the three SCZs.

SCZ 1**:**

$$n_-^1 \simeq 2\delta \tag{S33}$$
$$n_+^1 \simeq \frac{1}{2\delta}\left(1 - \frac{\Delta n}{2}\right)^2 \tag{S34}$$
$$V_1 \simeq -\Delta V + \log\left(\frac{2\delta}{1 - \Delta n/2}\right) \tag{S35}$$

SCZ lr**:**

$$n_-^l \simeq 2\delta \tag{S36}$$
$$n_+^r \simeq 2\alpha\delta \tag{S37}$$
$$V^l - V^r \simeq \log\left(\frac{2\alpha\delta}{n_+^l}\right) \simeq \log\left(\frac{2\delta}{n_-^r}\right) \tag{S38}$$

SCZ 2**:**

$$n_-^2 \simeq 2\alpha\delta \tag{S39}$$
$$n_+^2 \simeq \frac{1}{2\alpha\delta}(1 + \frac{\Delta n}{2})^2 \tag{S40}$$
$$V_2 \simeq \log\left(\frac{1 + \Delta n/2}{2\alpha\delta}\right) \tag{S41}$$

Analytical solution

This approximation reduces the number of unknowns and with the simple equations and boundary conditions that we have obtained, we can proceed straightforward to the full integration of the equations to obtain the remaining unknowns, n_+^l, n_-^r, V^l and V^r.

$$n_+^l = \frac{(1 - \Delta n/2)^2}{2\delta} - \frac{j_s + j_e}{4} \tag{S42}$$
$$n_-^r = \frac{j_s - j_e}{4} + \frac{(1 + \Delta n/2)^2}{2\alpha\delta} \tag{S43}$$
$$V^l = -\Delta V - \frac{j_e}{4\delta} + \log\left(\frac{2\delta}{1 - \Delta n/2}\right) \tag{S44}$$
$$V^r = \frac{j_e}{4\alpha\delta} - \log\left(\frac{2\alpha\delta}{1 + \Delta n/2}\right) \tag{S45}$$

Subtracting the last two equations (S44) and (S45) and making use of boundary condition equations (S38) with the expressions for n_+^l (S42) and n_-^r (S43) we have the following set of equalities,

$$\begin{aligned} V^l - V^r = \\ -\Delta V - \frac{j_e}{4\delta}\left(1 + \frac{1}{\alpha}\right) + \log\left(\frac{\alpha\,(2\delta)^2}{(1 - \Delta n/2)\,(1 + \Delta n/2)}\right) = \\ \log(2\alpha\delta) - \log\left(\frac{j_s + j_e}{4} - \frac{(1 - \Delta n/2)^2}{2\delta}\right) = \\ \log(2\delta) - \log\left(\frac{j_s - j_e}{4} - \frac{(1 + \Delta n/2)^2}{2\alpha\delta}\right) \end{aligned} \tag{S46}$$

The last two equations allows us to arrive to a relation between the electric and solute fluxes

$$j_e = \frac{1}{\alpha - 1}\left((\alpha + 1)j_s - \frac{4\Delta n}{\delta}\right) \tag{S47}$$

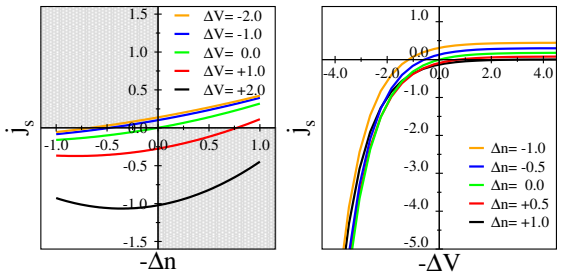

FIG. S2: Theoretical solute flux versus the concentration difference and the external voltage imposed between the two reservoirs, obtained from Eq. (S50).

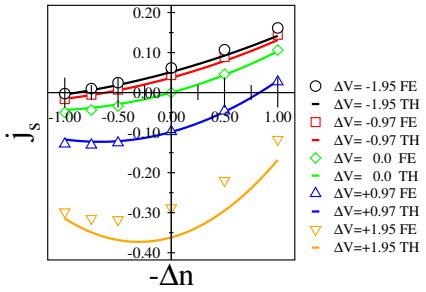

FIG. S3: Solute flux j_s versus salt concentration difference Δn: comparison of the FE solution of the full equations and the analytical approximation for large δ.

Or in a more general way, letting the concentrations of the reservoirs take any value n_L,n_R,

$$j_e = \frac{1}{\alpha - 1}\left((\alpha+1)j_s - \frac{2}{\delta}(n_L^2 - n_R)\right) \tag{S48}$$

Moreover, in the limit $\delta \gg 1$, the term $\frac{j_e}{4\delta}\left(1+\frac{1}{\alpha}\right)$ in equation (S46) can be neglected to obtain an explicit approximate expression for the solute flux in terms of the concentration imbalance of the reservoirs and the electric potential:

$$j_s = \frac{-2\Delta n}{\delta} - \frac{\alpha-1}{\alpha\delta}\left(1-\left(\frac{\Delta n}{2}\right)^2\right)\left(e^{+\Delta V} - \frac{2+\Delta n}{2-\Delta n}\right) \tag{S49}$$

or

$$j_s = \frac{n_L^2 - n_R^2}{\delta} - \frac{\alpha-1}{\alpha\delta} n_R\left(n_L e^{+\Delta V} - n_R\right) \tag{S50}$$

It is worth noting that in the regime $\Delta V \gg 1$, i.e. $eV/k_BT \gg 1$ in real units, the logarithms in equation (S46) become negligible compared to the ΔV contribution and we recover a linear regime $j_e = -4\delta\Delta V/\left(1+1/\alpha\right)$ where surface conduction dominates. This means that the exponential regime (S49) is only valid for low values of ΔV.

Comparison with the numerical solution of the full PNP equations

To check the validity of our simple analytical theory, we can make use of a finite elements (FE) method to solve the Nernst-Planck transport equations (S1) along with the electroneutrality condition. Instead of using the much more restrictive local electroneutrality ansatz that we used in the theory, here we can numerically solve the full Poisson equation instead.

$$\nabla^2 V = \begin{cases} -(1/\lambda_D)^2\left(n_+ - n_-\right)/2, & x < -1/2 \\ -(1/\lambda_D)^2\left(n_+ - n_- + \delta\right)/2, & -1/2 < x < 0 \\ -(1/\lambda_D)^2\left(n_+ - n_- - \alpha\delta\right)/2, & 0 < x < 1/2 \\ -(1/\lambda_D)^2\left(n_+ - n_-\right)/2, & 1/2 < x \end{cases}$$

This allows us to compare our theoretical predictions for large δ with the numerical solution of the full equations and also with the molecular dynamics simulations results. Since we are working in a regime of Debye length overlap we assume that the ion concentration will be approximately constant in the cross section of the channel and hence we will use 1D equations as we did in the analytical approach. As it can be observed in figure S3, the numerical solution of the complete equations validates the theory since for large δ the two are in excellent agreement.

Analytical solution for a symmetric channel

It is interesting to note that the complex osmotic phenomena that appear are advantageous due to the charge discontinuity in the channel. The performance of this device to produce asymmetric controllable flow can be compared to the one obtained by simple charged nanochannels. To visualize this, we can compare it against the behavior of a simple symmetric pore of Dukhin number δ. Following the same procedure as before, we obtain the expressions of the solute and electric flux for this simpler setup:

$$j_s = 2\delta\left[+\Delta V + \log\left(\frac{n_L}{n_R}\right) + \frac{n_L^2 - n_R^2}{2\delta^2}\right] \tag{S51}$$

$$j_e = 2\delta\left[-\Delta V - \log\left(\frac{n_L}{n_R}\right)\right] \tag{S52}$$

In figure S4 we compare the analytical solutions for the flux through a simple pore. In fact in the symmetric case we can get flux against the expected solute gradient. However, in this setup, a continuous current would be necessary to rectify the solute flux, which is not usually achievable in experiments, since it usually causes problems of polarization in the electrodes.

MOLECULAR DYNAMICS SIMULATIONS WITH AN IMPLICIT SOLVENT

By means of LAMMPS software [1] we perform molecular dynamics simulations in a setup like Fig. S1. A FCC lattice of fixed atoms was used to build the channel walls.

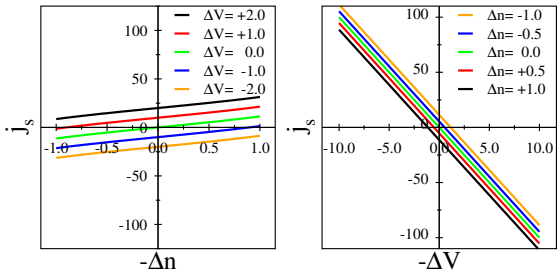

FIG. S4: Solute flux in terms of the osmotic gradient (left) and applied voltage (right) for a symmetric positively charged channel, obtained from Eq. (S51).

Water is modeled only in an implicit way, as a medium that has the dielectric permittivity of water $\epsilon_r = 80$. The interaction between the solute and the water molecules is mimicked by applying a Langevin thermostat on the ions [2]. The same damping time $\tau = 23$ fs – controlling the amplitude of the viscous drag in the Langevin model – is imposed for both species, to ensure that they have the same diffusion coefficient, with a value $D \approx 2 \times 10^{-9}$ m/s, close to experimental ones for typical microions. The atomic mass of the species is chosen to be $m_{n_+} = m_{n_-} = 39.1$ g/mol, and we consider monovalent ions. A Weeks–Chandler–Andersen potential, keeping only the repulsive part of the Lennard-Jones potential, was applied. All particles (ions and solid atoms) share the same size $\sigma = 3.74$ Å. Long-range Coulombic interactions were calculated by means of a particle-particle particle-mesh (PPPM) solver.

At each side of the junction charges were homogeneously distributed between the wall atoms at the surface, and the required amount of counterions to assure electroneutrality was placed in the vicinity of the walls. For the $\Delta n = 0$ case we used a single diode in contact with left and right reservoirs with the same concentration and periodic boundary conditions (PBC) in all space directions. A channel width equal to the Debye length $\lambda_D = 15$ Å was imposed to ensure Debye overlap. Each side of the diode in the x and y directions, as well as the reservoirs, had a length equal to $5\lambda_D$ to ensure that the concentration and voltage profiles reached a plateau value. To induce a voltage drop across the channel while keeping PBC, we imposed an electric field E_x to the system (in practice, by applying an electric force $F_x = qE_x$ on charged particles, with q the particle charge) [3, 4].

To avoid PBC problems in the $\Delta n \neq 0$ case, we constructed a double diode system such that along the x direction we had two diodes in series in such a way that the right reservoir of the first diode was also the left reservoir of the second diode and vice versa. We inverted the orientation of the second diode in such way that we can impose PBC in all space directions and from the same simulation we obtain the results for (Δn, $-\Delta V$) from the first channel and for (Δn,$+\Delta V$) from the second channel.

MOLECULAR DYNAMICS SIMULATIONS WITH AN EXPLICIT SOLVENT

Here we perform molecular dynamics simulations in a setup like Fig. 4b of the main text. The diode walls consisted of an array of graphene sheets with homogeneously distributed charges. The aim here was to build a realistic system in which water is explicitly included. The simulated systems contained $\sim$ 5000 water molecules, and five potassium and chloride atoms were typically present in each reservoir.

The AMBER96 force field [5] was used, with TIP3P water, and water-carbon interaction modeled by a Lennard-Jones potential between oxygen and carbon atoms, with parameters $\varepsilon_{\rm OC} = 0.114$ kcal/mol and $\sigma_{\rm OC} = 3.28$ Å. The values of the Lennard-Jones parameters for ions were taken as in reference [6] to avoid the formation of unrealistic clusters of ions in a very confined geometry. The simulations were carried out using LAMMPS [1]. Long-range Coulomb forces were computed using the particle-particle particle-mesh (PPPM) method. Water molecules were held rigid with the SHAKE algorithm. A time step of 2 fs was used. The positions of the carbon atoms were fixed. Water molecules and ions were kept at a constant temperature of 300 K using a Nosé-Hoover thermostat, applied only to the degrees of freedom perpendicular to the flow direction, with a damping time of 100 fs.

A channel width $h = 12$ Å was imposed, which provides a good Debye overlap for the Debye length $\lambda_D = 8$ Å used in this case. Each side of the diode in the x and y directions measured $3\lambda_D$, which gives almost flat concentration and voltage profiles on each side. The reservoirs and vacuum layers measured $\sim 10\lambda_D$. Besides the air-water interfaces, a vertical graphene wall is also included in the vacuum part of one side to assure that no evaporation occurs from one side to the other and hence water transfer can only occur through the channels.

Temporal evolution of the solute

Here we show the evolution of the amount of solute molecules in the left reservoir. This figure complements Fig. 4c showing that the flux of ions is negligible keeping its amount almost constant throughout the very long simulation (20 nanoseconds) and the much faster water flux dominates the dynamics.

* Electronic address: laurent.joly@univ-lyon1.fr

[1] S. Plimpton, *J. Comput. Phys.* **117**, 1 (1995).
[2] T. Schneider and E. Stoll, *Phys. Rev. B* **17**, 1302 (1978).
[3] P. S. Crozier, D. Henclerson, R. L Rowley, and D. D. Busath, *Biophys. J.* **81**, 3077 (2001).
[4] P. S. Crozier, R. L. Rowley, N. B. Holladay, D. Henderson and D. D. Busath, *Phys. Rev. Lett.* **86**, 2467 (2001).

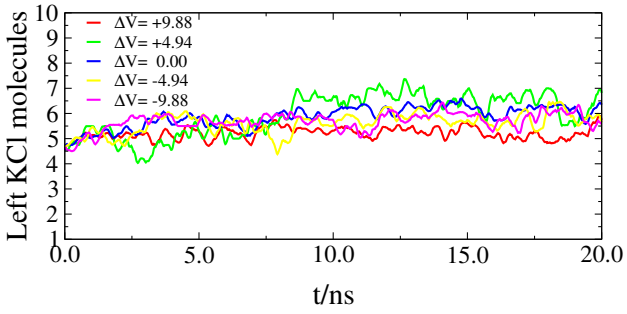

FIG. S5: Temporal evolution of the solute molecules after 20 ns during the same simulation as Fig. 4c in the main text.

[5] W. D. Cornell, P. Cieplak, C. I. Bayly, I. R. Gould, K. M. Merz, D. M. Ferguson, D. C. Spellmeyer, T. Fox, J. W. Caldwell and P. A. Kollman, *J. Am. Chem. Soc.* **117**, 5179 (1995).

[6] A. A. Chen and R. V. Pappu, *J. Phys. Chem. B* **111**, 11884 (2007).